NUMERICAL MODEL STUDY ON POLYHYDROXYALKANOATE PRODUCTION BY *CUPRIAVIDUS NECATOR*

NUMERICAL MODEL STUDY ON POLYHYDROXYALKANOATE PRODUCTION BY *CUPRIAVIDUS NECATOR*

By:

LI XU, B.Eng.

A Thesis Submitted to the School of Graduate Studies in Partial Fulfillment of the Requirements for the Degree of

Master of Applied Science

McMaster University

April 2021

McMaster University MASTER OF APPLIED SCIENCE (2021) Hamilton, Ontario (Civil Engineering)

TITLE: Numerical model study on polyhydroxyalkanoate production by *Cupriavidus necator*

AUTHOR: Li Xu, B. Eng.

SUPERVISOR: Dr. Younggy Kim

NUMBER OF PAGES: (ix, 43)

Abstract

Polyhydroxyalkanoates (PHAs) are biodegradable plastic synthesized by microorganisms from renewable carbon resources and they are promising substitutes for conventional fossil-fuel-based plastics due to their similar physical properties. Pure cultures of particular microorganisms are commonly used for industrial PHA production but high production costs due to requirements of sterile conditions and refined substrates hinder the mass production of PHAs. Thus, model development for PHA production by microbes is essential to investigate the PHA formation and microbial metabolisms for enhanced productivity and PHA contents. In the present study, a comprehensive numerical model has been developed and calibrated for the non-growth associated PHA production process by *Cupriavidus necator*. The model parameters were calibrated with 8 selected experimental studies and the simulation results show good agreement with experimental data. Two methods were used to conduct sensitivity analysis: the simple method and the overall relative sensitivity analysis method. Maximum specific residual biomass growth rate was the most sensitive parameter. The calibrated model was used to investigate fed-batch feeding strategies that optimize PHA accumulation by limited nutrient feeding in the PHA production phase. The simulation results showed limited phosphorous feeding accumulated more PHA than limited nitrogen feeding. The optimal feeding strategy was determined to be limited phosphorous feeding at 5% of initial phosphorous during the PHB production phase, yielding simulated 226.0 g/L PHB at the end of the 168-hour operation.

Contribution statement

The numerical model was developed by Abdelrahman Amer. Model calibration, sensitivity analysis for model parameters, and sample simulations for investigating the optimal feeding strategy were conducted by Li Xu.

Acknowledgment

I would like to firstly thank my supervisor, Dr. Younggy Kim who offered me the opportunity to grow professionally regarding research studies. I am truly grateful for all his patient guidance throughout all stages of my research. I would also like to thank the other members of my examination committee, Dr. Yiping Guo and Dr. Robin Zhao for their advice. I would like to thank the Natural Sciences and Engineering Research Council of Canada (Discovery Grants, RGPIN-2019-06747 and Discovery Accelerator Supplement, RGPAS-2019-00102) for the funding and support for my M.A.Sc. studies.

I would like to send my special thanks to Abdelrahman Amer. I feel grateful for his mentoring for my lab works and model studies. I appreciate his valuable suggestions and patient responses regarding my research work and my thesis. Also, I would like to thank Hui Guo for being my mentor and friend.

I would like to thank all my colleagues in the lab group who helped me in the lab, as well as friends in JHE 330 who offered me advice and supports. Finally, I would like to thank my parents for their supports and encouragement.

Table of Contents

List of Figures

List of Tables

List of Abbreviations

Polyhydroxyalkanoate	PHA
Short chain length PHAs	Scl-PHAs
Medium chain length PHAs	Mcl-PHAs
Polyhydroxybutyrate	PHB
Tricarboxylic acid cycle	TCA cycle
S	Soluble components
X	Particulate components
S_{S0}	Initial soluble substrate
S_{N0}	Initial ammonium plus ammonia nitrogen
S_{P0}	Initial phosphate phosphorous
X_{R0}	Initial residual biomass
X_{PHB0}	Initial PHB
X_{S0}	Initial slowly biodegradable particulate
X_{I0}	Initial inert particulate

1 Introduction

1.1 Background and research scope

Wastewater and sludge in wastewater treatment plants are now acknowledged as renewable resources because new material can be recovered from organic matters, nutrients, or solids contained in the sludge for secondary use [1]. Biodegradable plastic is one type of material that can be recovered from wastewater [2]. Plastic use is one of the environmental issues in these years because plastics in daily use are mostly derived from petroleum that is a non-renewable resource and non-biodegradable. For this reason, replacing synthetic fossil-fuel polymers with biodegradable plastics could reduce plastic pollution in the environment and cut down plastic production from fossil feedstock.

Polyhydroxyalkanoates (PHAs) are one type of bioplastics that are made from renewable carbon resources and biodegradable [3]. Figure 1-1 shows the general structural formula for PHA.

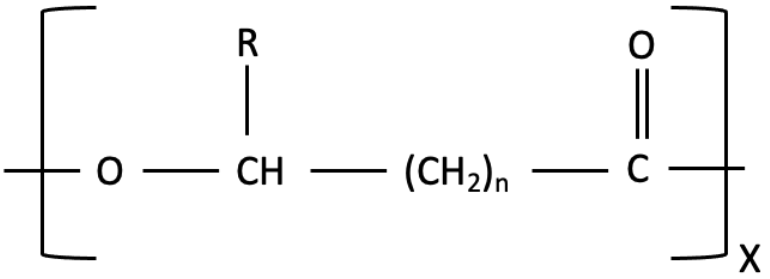

Figure 1-1:The general molecular structure of PHA[4]

A typical PHA molecule has x = 1,000–30,000 repeating units, and the molecule becomes polyhydroxybutyrate (PHB) when R is methyl and n=1[5]. PHB is the most well-known member of the family of PHA and was firstly identified in *Bacillus megaterium* by Lemoigne [5]–[7]. Based on the number of carbons in a PHA monomer, PHAs are categorized into either short chain length

PHAs (scl-PHAs) with 3-5 carbon atoms or medium chain length PHAs (mcl-PHAs) with 6-14 carbon atoms[8]. Scl-PHAs, such as PHB, are stiff and brittle, whereas mcl-PHAs are soft and elastic [2], [8].PHAs have great potential to replace conventional petroleum-based plastics not only because they are synthesized by utilizing renewable carbon resources from wastewater, but also because they have similar structural properties to those of polypropylene and have good biodegradability [9], [10].

The industrial PHA production uses either mixed culture or pure culture. The use of mixed culture requires an enrichment step before PHA accumulation to enrich microbes capable of producing PHA[11]. One enrichment method is applying a cyclic feast-famine condition in which the periods for substrate availability (feast) and substrate deficiency (famine) are alternated [12]. The feast phase drives both PHA storage and cell growth. During the famine phase, PHA producers survive with stored PHA as a carbon source and they become dominant in the culture after several cycles [12]. The use of pure culture for PHA production focuses on maximizing process productivity and high PHA content, managed by the type of microbial strains, cell density attained in cultivation, and the feeding mode [13]. PHA production using pure culture leads to high PHA content in the cell as high as 90% of their cell dry weight [13]. The focus of the present study is not the enrichment process in mixed culture, but the PHA accumulation process by pure culture.

There are more than 300 different microorganisms capable of producing PHA, but only a few bacteria can produce sufficient PHA for large-scale production [14]. These bacteria include *Cupriavidus necator*, *Alcaligenes latus*, *Azotobacter vinelandii*, *Pseudomonas oleovorans*, *Paracoccus denitrificans*, *Protomonas extorquens*, and recombinant *E. coli* [14]. PHA production is either growth-associated or non-growth-associated. For growth-associated

production, microbes such as *Alcaligenes latus* and *Paracoccus denitrificans* accumulate PHA in parallel to cell growth with sufficient nutrients [8]. For non-growth-associated PHA production, intensive PHA accumulation is triggered by depletion of growth-essential nutrients [15]. For example, *C. necator* synthesizes PHB with nutrient deficiencies [16] and utilizes different carbon sources, including glucose, fructose, glycerol, maltose, and CO_2/H_2 [17]–[21]. *Cupriavidus necator* is the most commonly used for non-growth-associated PHA production because it accumulates PHB up to 70% ~ 80% of cellular dry weight in an appropriate medium[16], [22], [23]. *Pseudomonas sp.* is another widely chosen non-growth-associated microbe in studies. Mozejko-Ciesielska et al. [24] reviewed that *Pseudomonas sp*. has been produced PHA in satisfactory amounts and at a low cost. Lee et al. [25] performed high cell density cultivation of *Pseudomonas putida* KT2442 from oleic acid coupled with phosphorus limitation and achieved a PHA content of 51.4%.

Optimization of the PHA production process on an industrial scale facilitates the replacement of petroleum-based plastic production with biodegradable plastic, which is a significant contribution to sustainability. Industrial PHA production by pure culture fermentation incurs high production costs due to requirements of sterile conditions in reactors and refined substrates in the medium[26]. Thus, model development for PHA production by microbes is essential to better investigate the PHA formation and microbial metabolisms for enhanced productivity. In the present study, a numerical model has been developed and calibrated for the non-growth associated PHB production process by *Cupriavidus necator*.

1.2 PHA production by pure culture triggered by nutrient limitation

In most PHA producing microorganisms, PHA accumulation is induced with excess carbon supply and limitation of important nutrients such as nitrogen and phosphorus [27]. The pathways of PHA synthesis are linked with the bacterium's central metabolic pathways such as the tricarboxylic acid cycle (TCA cycle), and these pathways share the common intermediate, acetyl-CoA[28]. The flow of acetyl-CoA to PHA biosynthetic pathways depends on the nutrient conditions [29]. With sufficient nutrient, a high amount of coenzyme A produced in the TCA cycle blocks the PHA synthesis pathway, so that acetyl-CoA flows mostly into the TCA cycle for energy production and cell growth; with limited nutrient, TCA cycle-related enzymes are inhibited, resulting in a low amount of coenzyme A and enabling acetyl-CoA to flows to PHA synthetic pathways for PHA accumulation [28],[29].

PHA production system by pure culture fermentation with nutrient limitation is characterized by a cell growth stage with nutrient availability and the following accumulation stage with depletion of one key nutrient [19], [30]. Oliveira-Filho et al.[31] evaluated the effects of nitrogen limitations in *B. sacchari* LFM101 growth and PHA biosynthesis using xylose as the sole source of carbon by conducting fed-batch experiments, and they observed that the PHB content achieved 61.70% under nitrogen limitation. El-Sayed et al.[32] performed two-stage batch fermentation of *Cupriavidus necator*. In the first stage, cells were cultivated with nitrogen sufficient medium for 24 hours and harvested by centrifugation. In the second stage, harvested cells are resuspended into a nitrogen-limited medium to promote PHB synthesis, yielding a PHB content of 51.84 %.

High cell density in the cell growth stage promotes high concentrations of PHA[5]. Wang and Lee [33] and Mozumder et al.[34] studied PHA production by *Cupriavidus necator* and maximized the

cell density by keeping nitrogen sufficient in the cell growth phase. Wang and Lee [33] maintained sufficient nitrogen source by using NH_4OH as pH control during the cell growth stage, and then nitrogen limitation was applied at 12 h by substituting NaOH solution for NH_4OH. A sharp increase in PHA production was observed, from 52% to 83%, after application of nitrogen limitation. Mozumder et al. [34] designed fed-batch fermentation of *Cupriavidus necator* by controlling substrate at the desired amount; when residual biomass was accumulated at a certain amount, nitrogen limitation was applied to trigger PHB production by stopping feeding nitrogen.

1.3 Kinetic modeling for PHA production by pure culture

Kinetic models for PHA production can be categorized as but not limited to formal kinetic models and metabolic models [35]. Formal kinetic models describe chemical kinetic relationships between substrates, products, and biomass by applying the Monod equation that links the substrate concentration to the specific growth rate[5], [35]. Metabolic models require detailed knowledge of metabolic chains, and incorporation of intermediates metabolism products and enzymes into the model components[36].

Metabolic models have been developed for getting insights into the effects of enzyme and metabolite concentrations on the PHA accumulation in microorganisms [37]. Lopar et al. [38] published a metabolic model for PHB production on glycerol by *C. necator* DSM 545. The mass balance equations were constructed based on 48 metabolic equations and there were 42 model components including key enzymes and intermediate metabolites. Although metabolic models reflect real metabolic situations in cells leading to more accurate prediction, the complexity of equation systems requires high computational demand. The formal kinetic models are based on macroscopic biochemical conversion, so they are faster to be established and solved. Špoljarić

et al.[39] commented they are less accurate but they are reliable for rough assessments of fermentation for laboratory research or industrial processes.

In the early stage of kinetic model development for PHA production, model components for formal kinetic models consist of substrate, biomass, and product (PHA)[35]. Later, Heinzle and Lafferty [40] divided the whole-cell biomass into intracellular storage (PHA) and residual biomass. Incorporation of substrate inhibition, cell density inhibition, product inhibition, as well as cell maintenance process into formal kinetic models was an incredible adaption because it reflects biological characteristics of the growth and production[35].

Luong [41] introduced carbon substrate inhibition (I_S) on specific growth rate by studying the inhibitory effect of butanol yeast growth, expressed as

$$I_S = \left(1 - \frac{S}{S_{max}}\right)^n \qquad (1\text{-}1)$$

where S is the substrate concentration, and n is an index of the inhibitory effect. Pérez Rivero et al.[19] explained high concentration of carbon substrate is likely to inhibit cell growth, especially if they are not adapted to the substrate.

Mulchandani et al. [42] introduced cell densities inhibition (I_C) on biomass growth rate expressed by logistic model:

$$I_C = 1 - \left(\frac{X}{X_{max}}\right)^{\alpha} \qquad (1\text{-}2)$$

Where α is an index of the inhibitory effect, and X is cell concentration. Experimental data from pure culture fermentation by Mozumder et al. [34] shows that cells cannot grow in an unlimited way because high cell density limits biomass growth on the substrate and PHB.

Nutrient inhibition term in the PHA production rate equation describes the non-growth associated PHA production. Mozumder et al. [34] expressed nitrogen inhibition (I_N) as

$$I_N = \frac{K_N}{K_N + S_N} \tag{1-3}$$

Shang et al [43] expressed phosphorus inhibition (I_P) as

$$I_P = \frac{K_P}{K_P + S_P} \tag{1-4}$$

where K_N and K_P are half-saturation of nitrogen (S_N) and phosphorus (S_P) respectively. With high concentrations of nitrogen and phosphorous, I_N and I_P tend to be low values inhibiting the PHA accumulation. Conversely, with a low concentration of nitrogen and phosphorous, I_N and I_P approach to 1, promoting PHA accumulation.

Marang et al.[44] incorporated PHB inhibition (I_{PHB}) term in PHB production rate equation to prevent unlimited accumulation of PHB:

$$I_{PHB} = 1 - \left(\frac{f_{(PHB)}}{f_{(PHB)}max}\right)^{\beta} \tag{1-5}$$

where β is the index for adjusting the relation between the PHB production rate and the amount of product, and $f_{(PHB)}$ is the ratio of PHB to residual biomass. Novak et al.[35] stated some strains were observed to stop PHA production when the mass fraction of PHA exceeded a threshold value since PHAs occupy the intracellular volume with accumulation.

The cell maintenance process is expressed by relating maintenance energy to the carbon substrate and product of storage (X_{STO}) [45]. Cell maintenance on the carbon substrate (r_{m_S}) and cell maintenance on X_{STO} ($r_{m_{STO}}$) are expressed as

$$r_{m_S} = m_{H,S} \frac{S_S}{K_S + S_S} \frac{S_O}{K_O + S_O} X_H \quad (1\text{-}6)$$

$$r_{m_{STO}} = m_{H,STO} \frac{K_S}{K_S + S_S} \frac{S_O}{K_O + S_O} \frac{X_{STO}/X_H}{K_{STO} + X_{STO}/X_H} X_H \quad (1\text{-}7)$$

where S_S is carbon substrate, S_O is oxygen, K_S and K_O are half-saturation of the carbon substrate and oxygen respectively, X_H is heterotrophic bacteria, $m_{H,S}$ is maintenance coefficient on the substrate, and $m_{H,STO}$ is maintenance coefficient on the product of storage.

1.4 Sensitivity analysis

Sensitivity analysis investigates the impact of small changes in nominal values of model parameters on model outputs and identifies the influential parameters in a model. The simplest method for sensitivity analysis is to quantify the percentage change in model output when changing one parameter at a time while keeping the others constant [46]. Then, the sensitivity of parameters can be ranked based on the change in model outputs. Marang et al. [44] identified significant parameters for their PHA producer growth model by measuring the change in time needed for the producer to reach 95% of the total biomass when the original value of each kinetic parameter is increased or decreased by 20%.

Another technique for sensitivity analysis is based on partial differentiation. The partial derivative of a dependent variable to a parameter is approximated by the first-order Taylor series [46]. The sensitivity of a particular parameter is expressed by the sensitivity coefficient ($\emptyset_i$) as

$$\emptyset_i = \frac{\partial y_i}{\partial x} \frac{x}{y_i} \quad (1\text{-}8)$$

where y_i is a particular dependent variable, x is the parameter, and the quotient $\frac{x}{y_i}$ is to normalize the coefficient to eliminate the effect of units. Partial derivatives are usually solved numerically

when models involve complex equations [46]. Vega et al.[30] and Mozumder et al.[34] quantified the sensitivity of model parameters of their kinetic models of PHA production based on $\emptyset_i$. They approximated the partial derivatives with the finite difference method, as shown in Equation (1-9)

$$\frac{\partial y_i(t)}{\partial x} = \frac{y(t, x + \Delta x) - y(t, x)}{\Delta x} \quad (1\text{-}9)$$

1.5 Research objectives

There are existing kinetic models for the PHA accumulation by pure cultures; however, they have some limitations to be used as comprehensive models for scaled-up PHA production because parameters were calibrated to fit specific cultivation conditions and the reported value of each parameter for comparison or initial guess is from the single published study. In existing model studies for pure culture, calibration is simply the procedure implemented for parameter estimation by applying estimation algorithms, but the estimated parameters are not compared to reported values from various studies, and the reliability of calibrated values for metabolic processes and kinetics of reactions is hardly investigated and discussed. The reliability of the model parameter is essential for a model because it assures the realistic prediction of production and provides a reliable process design.

The objectives of the present study are as follows:

(1) To develop a numerical model describing substrate consumption, cell growth, and PHB accumulation.

(2) To calibrate model parameters by fitting the model simulations with data from each published study and then calibrated values were compared to reasonable ranges of reported values in literature.

(3) To perform a sensitivity analysis to determine the most influential parameters affecting the model outputs.

(4) To apply the calibrated model to investigate optimal feeding strategy for maximizing PHB accumulation.

2 Numerical model development

2.1 Model development and calibration

The non-steady-state numerical model in this study described the production of PHB by *Cupriavidus necator* in batch or fed-batch reactor. There are 7 model components: soluble carbon substrate (S_S); ammonium plus ammonia nitrogen (S_N); phosphate phosphorus (S_P), residual biomass (X_R), slowly biodegradable particulate (X_S), inert particulate (X_I), and PHB (X_{PHB}). The units for carbon-based components are expressed in COD units; the unit for ammonium plus ammonia nitrogen concentration is expressed in gL^{-1} as N (nitrogen); the unit for phosphate phosphorus concentration is expressed in gL^{-1} as P (Phosphorous). Such units allow the model to be applied to studies with different substrates. The model consists of the following kinetic processes:

(1) PHB production on carbon substrate (r_1)

(2) cell growth on carbon substrate (r_2)

(3) cell growth on PHB (r_3)

(4) cell maintenance on carbon substrate (r_4)

(5) cell maintenance on PHB (r_5)

(6) cell decay (r_6)

(7) hydrolysis (r_7).

These kinetic processes are shown in Table 2-1

Table 2-1: Kinetic process expression and stoichiometric matrix of PHB production model

Kinetic process	Reaction rate equation	Soluble components			Particulate components			
		S_S	S_N	S_P	X_R	X_{PHB}	X_S	X_I
1.PHB production	$r_1 = k_{PHB}\frac{S_S}{K_S+S_S}\left(\frac{K_N}{K_N+S_N}+\frac{K_P}{K_P+S_P}-\left(\frac{K_N}{K_N+S_N}\frac{K_P}{K_P+S_P}\right)^{\gamma}\right)\left(1-\left(\frac{f_{(PHB)}}{f_{(PHB)}max}\right)^{\beta}\right)X_R$ (2-1)	$-\frac{1}{Y_{PHB/S}}$				1		
2.Cell growth on S_S	$r_2 = \mu_S\frac{S_S}{K_S+S_S}\frac{S_N}{K_N+S_N}\frac{S_P}{K_P+S_P}\left(1-\left(\frac{X_R}{X_{R\,max}}\right)^{\alpha}\right)X_R$ (2-2)	$-\frac{1}{Y_{X_R/S}}$	$-i_{NBM}$	$-i_{PBM}$	1			
3. Cell growth on X_{PHB}	$r_3 = \mu_{PHB}\frac{K_S}{K_S+S_S}\frac{S_N}{K_N+S_N}\frac{S_P}{K_P+S_P}\frac{f_{(PHB)}}{K_{PHB}+f_{(PHB)}}\left(1-\left(\frac{X_R}{X_{R\,max}}\right)^{\alpha}\right)X_R$ (2-3)		$-i_{NBM}$	$-i_{PBM}$	1	$-\frac{1}{Y_{X_R/PHB}}$		
4.Maintenance on S_S	$r_4 = m_S\frac{S_S}{K_S+S_S}X_R$ (2-4)	-1						
5.Maintenance on X_{PHB}	$r_5 = m_{PHB}\frac{K_S}{K_S+S_S}\frac{f_{(PHB)}}{K_{PHB}+f_{(PHB)}}X_R$ (2-5)					-1		
6.Decay	$r_6 = b\frac{K_{PHB}}{K_{PHB}+f_{PHB}}X_R$ (2-6)		$i_{NBM}-f_I i_{NBM}$	$i_{PBM}-f_I i_{PBM}$	-1		$1-f_I$	f_I
7.Hydrolysis	$r_7 = k_H\frac{X_S/X_R}{K_X+(X_S/X_R)}X_R$ (2-7)	1					-1	

The present model is based on ASM 3[47] featuring in Monod equation with some modifications. The adaption includes cell growth on the substrate, cell density inhibition in biomass growth, PHA accumulation inhibition in PHA production, as well as cell maintenance on substrate and PHA, based on the model study by Mozumder et al. [17]

The assumptions made for the model are as follow:

(1) The total biomass (X) was assumed to consist of residual biomass (X_R) and PHB (X_{PHB}).

(2) S_S represents a single carbon substrate such as glucose.

(3) f_{PHB} is derived from PHB content of total biomass, expressed as

$$f_{PHB} = \frac{PHA\ content}{1-PHA\ content} \quad (2\text{-}8)$$

(4) The oxygen concentration in the process was assumed to be in a non-limiting amount, so dissolved oxygen is not included in the model components.

(5) The temperature is maintained at 30℃.

(6) pH is set to be 7.0.

(7) The carbon substrate inhibition is not taken into account in the model.

The non-steady-state mass balance differential equations were built based on kinetic reaction rate expressions and stoichiometric matrix in Table 2-1. Differential equations were numerically approximated by the Crank-Nicolson method, and they were solved by fixed-point iteration. The convergence criteria of fixed-point iteration is $|x_n-x_{n-1}| <10^{-5}$, where x_n is n^{th} root and $x_{n-1}$is n-1^{th} root. The numerical model was programmed in Visual Basic for Applications (VBA).

2.2 Model calibration with published experimental results

Model kinetic parameter and stoichiometric coefficients were calibrated by fitting the model to published data from the literature. Experimental data from literature were extracted from images of figures by using the data extracting software WebPlotDigitizer (Version 4.4, USA). However, the data extracting software cannot assure 100% accuracy due to human error when selecting points on an image, especially the initial point of biomass and PHA which close to zero. Change of initial value of biomass for model simulation from 0.01 to 0.1 g/L could make a non-negligible difference in simulation results of model components. Thus, reasonable assumptions for the initial value of biomass were made based on the experimental data.

In the studies used for calibration of the present model, *C. necator* was used as a microorganism and cultivated in either batch or fed-batch reactors under controlled conditions at 30℃ and neutral pH. Oxygen was supplied with sufficient amount to ensure the process was not limited by levels of dissolved oxygen. Table 2-2 shows operational conditions, initial conditions for substrates and biomass, and maximum PHA content for selected studies. The initial inert particulates and slowly biodegradable particulates are set to be zero.

Table 2-2: Operational conditions, initial conditions, and maximum PHA content for selected experimental works

Selected experimental work	Reactor	Organic substrate (S_{S0})	Nutrient		Biomass		Operation time	pH	Max. PHB content
			S_{N0}	S_{P0}	X_{PHB0}	X_{R0}			
[58]	Batch	42.24 $\frac{g-COD}{L}$ glucose	2.41 $\frac{g-N}{L}$	0.58 $\frac{g-P}{L}$	0.13 $\frac{g-COD}{L}$	0.74 $\frac{g-COD}{L}$	23 hr	7.0	20 %
[48]	Batch	24.35 $\frac{g-COD}{L}$ glycerol	0.42 $\frac{g-N}{L}$	1.13 $\frac{g-P}{L}$	0.05 $\frac{g-COD}{L}$	0.85 $\frac{g-COD}{L}$	36 hr	6.8	65 %
[49]	Batch	16.00 $\frac{g-COD}{L}$ glucose	0.38 $\frac{g-N}{L}$	3.03 $\frac{g-P}{L}$	0.37 $\frac{g-COD}{L}$	0.11 $\frac{g-COD}{L}$	52 hr	6.8	67 %
[19]	Batch	24.35 $\frac{g-COD}{L}$ glycerol	0.21 $\frac{g-N}{L}$	1.12 $\frac{g-P}{L}$	0.08 $\frac{g-COD}{L}$	0.07 $\frac{g-COD}{L}$	92 hr	6.8	73 %
		36.52 $\frac{g-COD}{L}$ glycerol					104 hr		79 %
[50]	Fed-batch	60.87 $\frac{g-COD}{L}$ glycerol	0.6 $\frac{g-N}{L}$	1.12 $\frac{g-P}{L}$	0.03 $\frac{g-COD}{L}$	0.75 $\frac{g-COD}{L}$	120 hr	6.8	87 %
[13]	Batch	40.21$\frac{g-COD}{L}$ glucose	0.34 $\frac{g-N}{L}$	2.04 $\frac{g-P}{L}$	0 $\frac{g-COD}{L}$	0.1 $\frac{g-COD}{L}$	72 hr	6.8	90 %
[16]	Batch	60.87 $\frac{g-COD}{L}$ glycerol	1.79 $\frac{g-N}{L}$	1.93 $\frac{g-P}{L}$	0.74 $\frac{g-COD}{L}$	0.38 $\frac{g-COD}{L}$	32 hr	6.8	50 %
[17]	Fed-batch	12.8 $\frac{g-COD}{L}$ glucose	0.6 $\frac{g-N}{L}$	3 $\frac{g-P}{L}$	0 $\frac{g-COD}{L}$	0.1 $\frac{g-COD}{L}$	66.5 hr	6.8	76 %
		17.4 $\frac{g-COD}{L}$ glycerol					45 hr		70 %

In model calibration study with each published study, the initial guess of parameters was made based on reported values in literature shown in Table 2-3.

Table 2-3: Model parameters and their reported values from literature at 30℃.

Parameter	Reported range from literature	Reference	Suggested value for this model
Max. specific X_R growth rate on S_S (μ_S)	0.11~0.46 h^{-1}	[16], [17], [19], [22], [30], [39], [43], [48], [49], [51]–[55]	0.3 h^{-1}
Max. specific X_R growth rate on PHB (μ_{PHB})	0.08 ~0.18 h^{-1}	[13], [17], [54]	0.18 h^{-1}
Half-saturation constant on S_S (Ks)	1.2 ~ 1.92 $\frac{g-COD}{L}$	[17], [19], [30], [43], [54]	1.9 $\frac{g-COD}{L}$
Saturation constant on PHB (K_{PHB})	0.18~0.26 $\frac{gPHB-COD}{gX_R-COD}$	[17], [19], [54]	0.25 $\frac{gPHB-COD}{gX_R-COD}$
Nitrogen affinity constant (K_N)	0.01 ~0.39 $\frac{g-N}{L}$	[17], [19], [22], [30], [52], [54]	0.25 $\frac{g-N}{L}$
Phosphorous affinity constant (K_P)	10^{-5} $\frac{g-P}{L}$	[47]	0.25 $\frac{g-P}{L}$
Maintenance coefficient on S_S (m_S)	0.015 ~ 0.048 h^{-1}	[17], [30], [43], [49], [52]	0.015 h^{-1}
Maintenance coefficient on PHB (m_{PHB})	0.0044 h^{-1}	[45]	0.0044 h^{-1}
Max. specific PHB production rate (k_{PHB})	0.034~0.23 h^{-1}	[17], [19], [22], [39], [43], [53]–[55] [52]	0.18 h^{-1}
Decay rate coefficient (b)	0.0018 ~0.02 h^{-1}	[47], [56], [20]	0.01 h^{-1}
Max. PHB to X_R ratio ($f_{(PHB)}^{Max}$)	1.22 ~ 11.5 $\frac{gPHB-COD}{gX_R-COD}$	[22], [48], [17],[49], [51], [39], [17], [19] [54], [53],[13], [20], [55]	4 $\frac{gPHB-COD}{gX_R-COD}$
Max. residual biomass ($X_{R\ max}$)	96.28 ~98 $\frac{g-COD}{L}$	[17], [43]	96.28 $\frac{g-COD}{L}$
Max. hydrolysis rate (k_H)	0.125 h^{-1}	[47]	0.125 h^{-1}
Hydrolysis affinity constant (K_X)	0.03 $\frac{g-COD}{g-COD}$	[47]	0.03 $\frac{g-COD}{g-COD}$
Yield coefficient for growth on S_S ($Y_{X_R/S}$)	0.4 ~0.65 $\frac{gX_R-COD}{gS_S-COD}$	[19], [20], [30], [43], [49], [52]–[54]	0.6 $\frac{gX_R-COD}{gS_S-COD}$
Yield coefficient for PHB ($Y_{PHB/S}$)	0.4 ~0.75 $\frac{gPHB-COD}{gS_S-COD}$	[13], [19], [20], [22], [30], [39], [43], [49]–[51], [53]–[55]	0.4 $\frac{gPHB-COD}{gS_S-COD}$
Yield coefficient for growth on PHB ($Y_{X_R/PHB}$)	0.51 ~ 0.74 $\frac{gX_R-COD}{gPHB-COD}$	[17], [51]	0.74 $\frac{gX_R-COD}{gPHB-COD}$
Fraction of X_I (f_I)	0.2 $\frac{g-COD}{g-COD}$	[47]	0.2 $\frac{g-COD}{g-COD}$
Nitrogen content of biomass (i_{NBM})	0.06 ~ 0.19 $\frac{g-N}{g-COD}$	[19], [30], [39], [49], [52], [54], [55]	0.1 $\frac{g-N}{g-COD}$
Nitrogen content of X_I (i_{NXI})	0.06 $\frac{g-N}{g-COD}$	[47]	0.06 $\frac{g-N}{g-COD}$
Phosphorus content of biomass (i_{PBM})	0.03 ~ 0.036 $\frac{g-P}{g-COD}$	[22], [43]	0.03 $\frac{g-P}{g-COD}$
Phosphorus content of X_I (i_{PXI})	0.03 ~ 0.036 $\frac{g-P}{g-COD}$	[22], [43]	0.03$\frac{g-P}{g-COD}$
Cell density inhibition index (α)	5.8	[17], [42]	5.8
PHB production inhibition index (β)	3.85	[17], [57]	3.85
Constant to keep specific PHB production rate less than 1 (γ)	0.95	this study	0.95

Model parameters were then calibrated to fit experimental data by trial and error. The calibrated parameters were compared to the range of reported values. Then, a unified value for each parameter was estimated based on the model.

2.3 Sensitivity analysis

Two sensitivity analysis methods were performed to identify the most sensitive parameters affecting the model outputs. One method is the simple method. A parameter is changed by 1% of the default value and the percentage change of the model output was determined at a specific arbitrary time. Maximum X_{PHB}, Maximum X_R, the time required for achieving maximum X_{PHB}, and the time required for achieving maximum X_R are the model outputs for the analysis.

The other method is the overall relative sensitivity analysis based on partial differentiation of model output to the parameter. The relative sensitivity function used in this study is adapted from Mozumder et al. [17]. The relative sensitivity function is dimensionless and the overall sensitivity of different parameters over a certain period was determined. The relative sensitivity function ($\partial_{Rf}(t)$) of variable y towards parameter θ at time instant t is defined as

$$\partial_{Rf}(t) = \frac{\partial y_i(t)}{\partial \theta}\frac{\theta}{y_i(t)} = \frac{y(t,\theta+\Delta\theta)-y(t,\theta-\Delta\theta)}{2\Delta\theta}\frac{\theta}{y_i(t)} \quad (2\text{-}9)$$

$\Delta\theta$ is the change of parameter, which is 1% of θ.

The overall sensitivity ∂ is defined as

$$\partial = \frac{\sum_{i=1}^{t}\frac{\partial y_i(t)}{\partial \theta}\frac{\theta}{y_i(t)}}{n} \quad (2\text{-}10)$$

where n is the number of virtual measurements, and t is the operation period.

The criteria of sensitive parameters for the simple method is the change of the model outputs greater than 0.1%, and the criteria for overall sensitivity is $\partial > 0.1$. The simulation scenario in the sensitivity analysis is the batch cultivation over 60 hours. The initial values for model components are shown in Table 2-4.

Table 2-4:Initial conditions for sensitivity analysis

Component	S_{S0}	S_{N0}	S_{P0}	X_{PHB0}	X_{R0}	X_{S0}	X_{I0}
Concentration	$32\ \frac{g-COD}{L}$	$0.53\ \frac{g-N}{L}$	$1.12\ \frac{g-P}{L}$	$0.0167\ \frac{g-COD}{L}$	$0.142\ \frac{g-COD}{L}$	0	0

2.4 Model applications

The calibrated model was applied to investigate the nutrient feeding strategy that maximizes PHB production by maintaining residual cell growth during the PHB production phase, based on Schmidt et al.[23]. The process is designed as fed-batch cultivation with cell recycle for 7 days (168 hr). The initial conditions of fresh medium and particulates for the simulations are shown in Table 2-5.

Table 2-5:Initial condition for the simulations

Component	S_{S0}	S_{N0}	S_{P0}	X_{PHB0}	X_{R0}	X_{S0}	X_{I0}
Concentration	$16\ \frac{g-COD}{L}$	$0.6\ \frac{g-N}{L}$	$1.12\ \frac{g-P}{L}$	$0.0167\ \frac{g-COD}{L}$	$0.142\ \frac{g-COD}{L}$	0	0

Whenever S_S is consumed by 99% of the initial S_S, 25% of the culture medium is removed and replaced with the fresh medium; the biomass in the removed medium is recycled back to the bioreactor to maintain high cell density. Residual cell growth is maintained during the PHB production phase by supplying a limited amount of a key nutrient during repeated fed-batch feedings of fresh medium. The concentration of S_N or S_P in the fresh medium for the following

repeated fed-batch feeding depends on simulation scenarios. In 1st scenario, the amount of nitrogen is at a limited level, varying from 10% to 70% of S_{N0}, and S_P is the same as S_{P0}. In 2nd scenario, the amount of phosphorous is at a limited level, varying from 1% to 7% of initial S_P, and S_N is kept the same as S_{N0}.

3 Results and discussion

3.1 Model calibration with published experimental results

The present model was calibrated with 8 published studies for PHA production by *C. necator* and fit the experimental data well. Model parameters for each experimental study were calibrated within the reported range and were kept as unified as possible among selected studies.

Figure 3-1 shows the model prediction for the short-term batch culture of *Cupriavidus necator* on glucose, conducted by Belfares et al [58]. The fitness of the model outputs to experimental data proves the model can effectively describe the cell growth phase of non-growth-associated PHB production. With the availability of nitrogen throughout the operation, the predicted amount of PHB accumulated at the end of the period is at an insignificant level that is less than 3 g/L, comparing to residual biomass (X_R) which is around 10 g/L.

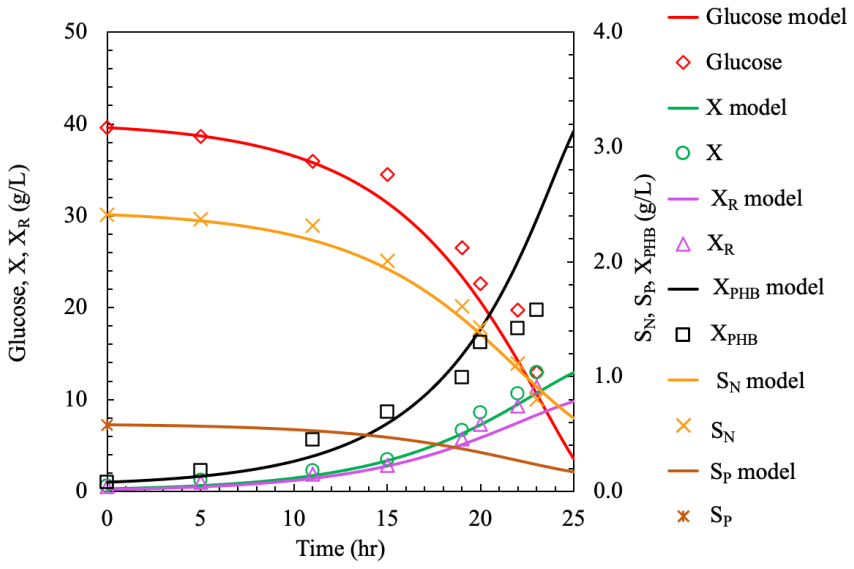

Figure 3-1:Model calibration with experimental data of Belfares et al. [58].

Figure 3-2 shows model fitting with the experimental data of Gahlawat and Soni [48]. They conducted batch cultivation for PHB production by *Cupriavidus necator* on glycerol. Predicted glycerol consumption, biomass growth, and PHB accumulation had a good agreement with the data.

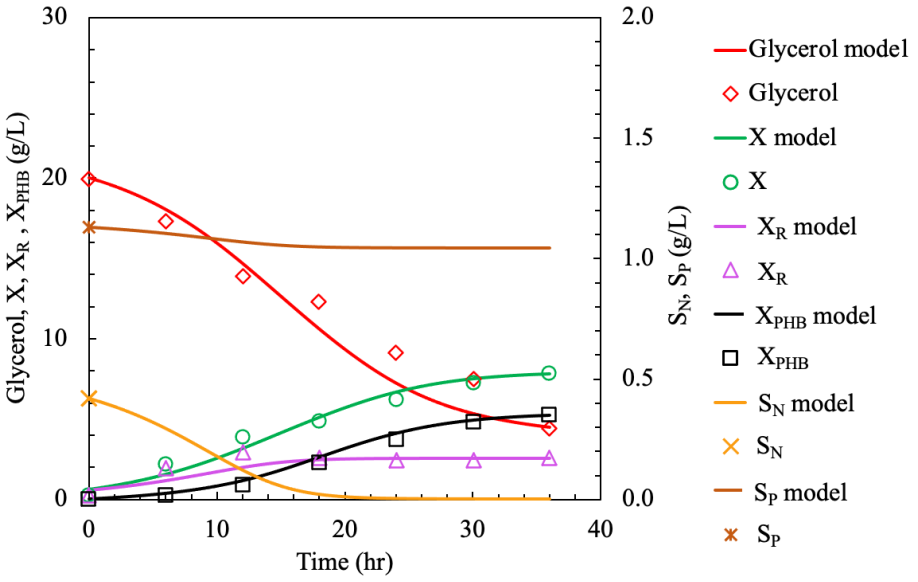

Figure 3-2: Model calibration with experimental data of Gahlawat and Soni [48]

Suggested values for the model parameters were estimated by taking the most frequently appeared values obtained from calibration studies. Calibrated μ_S and k_{PHB} vary among studies because they are dependent on experimental conditions or experimentally measured specific growth rate and PHB production rate. For example, Gahlawat and Soni [48] measured the maximum growth rate of *C. necator* by utilizing glycerol ranged from 0.26 to 0.28 h^{-1}. $f_{(PHB)}^{Max}$ varies among studies because it is determined based on PHB content (%) measured in the experiments. The value of $f_{(PHB)}^{Max}$ for the model was estimated as 4 derived from a PHB content of 80% since *C. necator* can accumulate PHB up to 80% of the dry weight of biomass[23]. $Y_{PHB/S}$ varies from 0.4 to 0.7

because it depends on the experimental accumulation of PHA. Table 3-1 lists the calibrated kinetic and stoichiometric parameter values.

Table 3-1: Model calibration results with published studies

Figure	3-1	3-2	3-3	S1A	S1B	S2	S3	S4	S5A, B	S5C	Suggested value in this study
Data Reference	[58]	[48]	[49]	[19]		[50]	[13]	[16]	[17]		
μ_S (h^{-1})	0.3	0.26	0.3	0.3		0.3	0.3	0.14	0.4		0.3
μ_{PHB} (h^{-1})	0.18							0.1	0.18		0.18
Ks ($\frac{g-COD}{L}$)	1.9										1.9
K_{PHB} ($\frac{gPHB-COD}{gX_R-COD}$)	0.25										0.25
K_N ($\frac{g-N}{L}$)	0.25		0.05	0.25							0.25
K_P ($\frac{g-P}{L}$)	0.25										0.25
m_S (h^{-1})	0.015										0.015
m_{PHB} (h^{-1})	0.0044										0.0044
k_{PHB} (h^{-1})	0.12	0.18						0.23	0.13	0.18	0.18
b (h^{-1})	0.01								0.02		0.01
$f_{(PHB)}^{Max}$ ($\frac{gPHB-COD}{gX_R-COD}$)	4	2.5	2.03	4		6.9		9	3	2.3	4
$X_{R\ max}$ ($\frac{g-COD}{L}$)	96.28										96.28
k_H (h^{-1})	0.125										0.125
K_X ($\frac{g-COD}{g-COD}$)	0.03										0.03
$Y_{X_R/S}$ ($\frac{gX_R-COD}{gS_S-COD}$)	0.6										0.6
$Y_{PHB/S}$ ($\frac{gPHB-COD}{gS_S-COD}$)	0.4	0.7		0.4		0.4	0.5	0.4			0.4
$Y_{X_R/PHB}$ ($\frac{gX_R-COD}{gPHB-COD}$)	0.74										0.74
f_I ($\frac{g-COD}{g-COD}$)	0.2										0.2
i_{NBM} ($\frac{g-N}{g-COD}$)	0.11	0.15	0.1						0.06	0.1	0.1
i_{NXI} ($\frac{g-N}{g-COD}$)	0.06										0.06
i_{PBM} ($\frac{g-P}{g-COD}$)	0.03										0.03
i_{PXI} ($\frac{g-P}{g-COD}$)	0.03										0.03
α	5.8										5.8
β	3.85										3.85
γ	0.95										0.95

Calibrated K_N is 0.25 g $N.L^{-1}$ for the most selected studies, except that K_N is 0.05 g $N.L^{-1}$ for Marudkla et al. [49]. Marudkla et al. [49] performed batch cultivation of PHB production by *C. necator* on glucose. As shown in Figure 3-3, the model is calibrated with the data by setting K_N to 0.05 g $N.L^{-1}$. With such value, modeled PHB accumulation could fit the measured PHB accumulation that started after 16 hours.

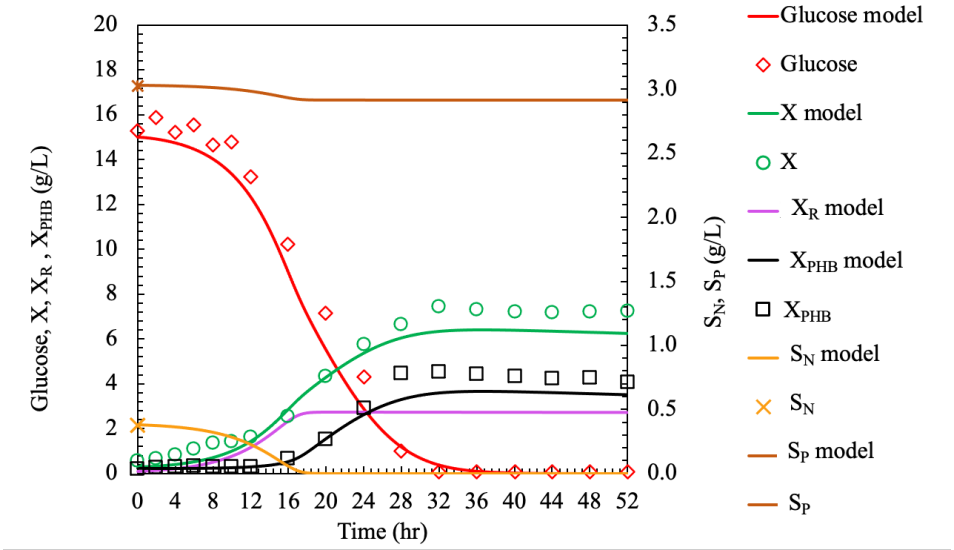

Figure 3-3: Model calibration for experimental data of Marudkla et al. [49]

3.2 Sensitivity analysis

The sensitivity of parameters to model output was evaluated by two sensitivity analysis methods that are the simple method and the overall relative sensitivity analysis method. Table 3-2 shows the parameter sensitivity analysis results by two methods. Bold fonts indicate the values above the criteria of sensitive parameters.

Table 3-2: Parameter sensitivity results by the simple method and the overall relative sensitivity analysis with respect to model outputs.

Parameter (θ)	The simple method				The overall relative sensitivity analysis	
	Increase in Max. X_{PHB} with 1% increase of θ	Increase in the required time for max. X_{PHB} with a 1% increase of θ	Increase in Max. X_R with 1% increase of θ	Increase in the required time for max. X_R with a 1% increase of θ	∂ for X_{PHB} with $\Delta\theta = 1\%\theta$	∂ for X_R with $\Delta\theta = 1\%\theta$
μ_S	0.04%	**-0.57%**	0.00%	**-1.09%**	**0.888**	**0.751**
μ_{PHA}	-0.02%	0.00%	0.01%	**-0.10%**	-0.018	0.018
Ks	-0.03%	**0.11%**	0.00%	**0.10%**	**-0.110**	-0.032
K_{PHB}	0.00%	0.00%	-0.01%	0.00%	-0.015	-0.024
$Y_{X_R/S}$	**0.39%**	**0.11%**	0.00%	0.00%	**0.202**	0.003
K_N	0.00%	**0.11%**	-0.01%	**0.79%**	**-0.127**	**-0.274**
K_P	0.00%	**0.11%**	0.00%	**0.30%**	-0.071	**-0.139**
m_S	-0.05%	0.00%	0.00%	**0.10%**	-0.023	0.000
m_{PHB}	-0.01%	0.00%	0.00%	0.00%	-0.007	0.000
$Y_{PHB/S}$	**1.00%**	**0.34%**	0.01%	**-0.20%**	**0.500**	0.006
$Y_{X_R/PHB}$	0.04%	0.00%	0.00%	**0.10%**	0.054	0.001
k_{PHB}	0.05%	**-0.46%**	0.00%	**0.30%**	**0.531**	0.016
$f_{(PHB)}^{max}$	0.00%	0.00%	0.00%	**0.10%**	0.002	0.000
β	0.00%	0.00%	0.00%	**0.10%**	0.001	0.000
b	-0.01%	0.00%	-0.01%	0.00%	-0.037	-0.028
γ	0.02%	**-0.23%**	0.00%	**0.20%**	**0.218**	0.006
f_I	0.00%	0.00%	-0.01%	0.00%	0.002	-0.003
i_{NBM}	**0.44%**	**0.34%**	**-0.95%**	**-0.40%**	**0.247**	**-0.572**
i_{NXI}	0.00%	0.00%	-0.01%	0.00%	0.002	-0.003
i_{PBM}	0.00%	0.00%	0.00%	0.10%	-0.001	-0.003
$_{iPXI}$	0.00%	0.00%	0.00%	0.00%	0.000	0.000
α	0.00%	0.00%	0.00%	0.00%	0.000	0.000
$X_{R\ max}$	0.00%	0.00%	0.00%	0.00%	0.000	0.000
K_X	0.00%	0.00%	0.00%	0.00%	0.000	0.000
k_H	0.00%	0.00%	0.00%	0.00%	0.000	0.000

The parameters μ_S, k_{PHB}, $Y_{X_R/S}$, $Y_{PHB/S}$, Ks, K_N, K_P, i_{NBM}, and γ were found sensitive based on the overall relative sensitivity. μ_S has the highest overall sensitivity and positive correlation to PHB and residual biomass. It is also sensitive to accumulation time for maximum PHB and residual biomass with a 1% increase since the time for accumulating maximum PHB and growing maximum residual biomass is shortened by 0.57% and 1.09% respectively. The reported range of

μ_S is wide, from 0.11 to 0.46 h^{-1}, so it is important to carefully measure the specific growth rate experimentally when estimating μ_S for a specific bioreactor.

k_{PHB} is sensitive to PHB accumulation and is positively correlated. The time for accumulating maximum PHB is shortened by 0.46% but the time for growing maximum residual biomass is prolonged by 0.3% with a 1% increase of k_{PHB}. k_{PHB} ranges from 0.034 to 0.23 h^{-1}, depending on experimental conditions. Thus, increasing the PHB production rate to the high end of the reported range accelerates PHB production and makes PHB production more dominant than cell growth.

$Y_{X_R/S}$ is sensitive to PHB accumulation and time for accumulating maximum PHB with positive correlation. 1% increase of $Y_{X_R/S}$ increases maximum PHB accumulation by 0.39% but increases the time for accumulating maximum PHB by 0.11%. The positive correlation of PHB accumulation with $Y_{X_R/S}$ can be explained by higher cell density leading to a higher amount of PHB. $Y_{PHB/S}$ has higher sensitivity to PHB accumulation than $Y_{X_R/S}$ because the yield of PHB over the substrate is directly related to the formation of PHB. It also shortens the time for growing maximum residual biomass. Thus, calibrating $Y_{PHB/S}$ is in the higher priority than $Y_{X_R/S}$. $Y_{X_R/S}$ and $Y_{PHB/S}$ can be calculated based experimentally measured PHB and biomass formation and substrate consumption, so comparing the estimated value to experimentally determined value can enhance the accuracy of the model prediction.

K_N is sensitive to PHB and residual biomass accumulation with negative correlation, corresponding to its positive correlation with time for accumulating maximum PHB and residual biomass. K_P is sensitive to residual biomass accumulation with negative correlation, as well as sensitive to time for accumulating maximum PHB and time for growing maximum residual

biomass with positive correlation. K_N has a wide reported range from 0.01 to 0.39 $\frac{g-N}{L}$, and the studies for estimating K_P are limited, so experimental studies are essential to determine the initial guess for K_N and K_P. Ks is sensitive to PHB accumulation with negative correlation, as well as sensitive to time for accumulating maximum PHB and time for growing residual biomass with positive correlation. K_S has a narrow reported range from 1.2 ~ 1.92 $\frac{g-COD}{L}$, so the estimated value can be directly used.

i_{NBM} is sensitive to all model outputs evaluated by both methods. It is positively correlated with maximum PHB accumulation and its required time but negatively correlated with maximum residual biomass and its required time. Since i_{NBM} has a wide range from 0.06 ~ 0.19 $\frac{g-N}{g-COD}$, it is necessary to verify the estimated value by calculating the ratio of nitrogen uptake rate to cell growth rate [49].

γ is sensitive to PHB accumulation with a positive correlation. 1% increase in γ shortens the time for accumulating maximum PHB but prolongs the time for growing maximum residual biomass. γ is an index in the nutrient inhibition term of PHB production rate, so studying the value of γ with experimental data helps understand the relationship between PHB production and nutrient inhibition and makes simulation results more reliable.

The results of parameter sensitivity evaluated by the two methods are not completely consistent. In the simple method, $Y_{PHB/S}$ is the most sensitive to PHB accumulation, and i_{NBM} is the most sensitive to X_R. In the overall relative sensitivity analysis method, μ_S is the most sensitive to PHB and X_R. The reason for the inconsistency is that the overall sensitivity analysis method considers the sensitivity of parameters over the whole period and takes the average, but the simple method

only evaluates sensitivity at a time instant when maximum amount is realized. Thus, required time for maximum amount accumulation is the supplement model output to provide with the full picture of parameter sensitivity in the simple method.

3.3 Model applications

The simulations for PHB accumulation over a 7-day operation for two scenarios are illustrated in Figure 3-4. In 1st scenario (Figure 3-4 A), the amount of PHB accumulated at a different level of nitrogen concentration starts to differentiate around 68 hours. In 2nd scenario (Figure 3-4 B), the amount of PHB accumulated at a different level of phosphorous starts to differentiate around 72 hours. Hence, at least 68 hr of operation with limited nitrogen and 72 hr of operation with limited phosphorous are required for maximizing PHB accumulation by maintaining residual cell growth in the production phase. The increase of nutrient amount in fed-batch feeding medium leads to a higher PHB accumulation rate, so the time for accumulating a particular amount of PHB could be shortened with increasing of nutrient amount. The optimal feeding amount of nutrient at which PHB is maximized at the end of the operation is 40% S_{N0} for nitrogen-limited medium and 5% S_{P0} for phosphorous limited medium.

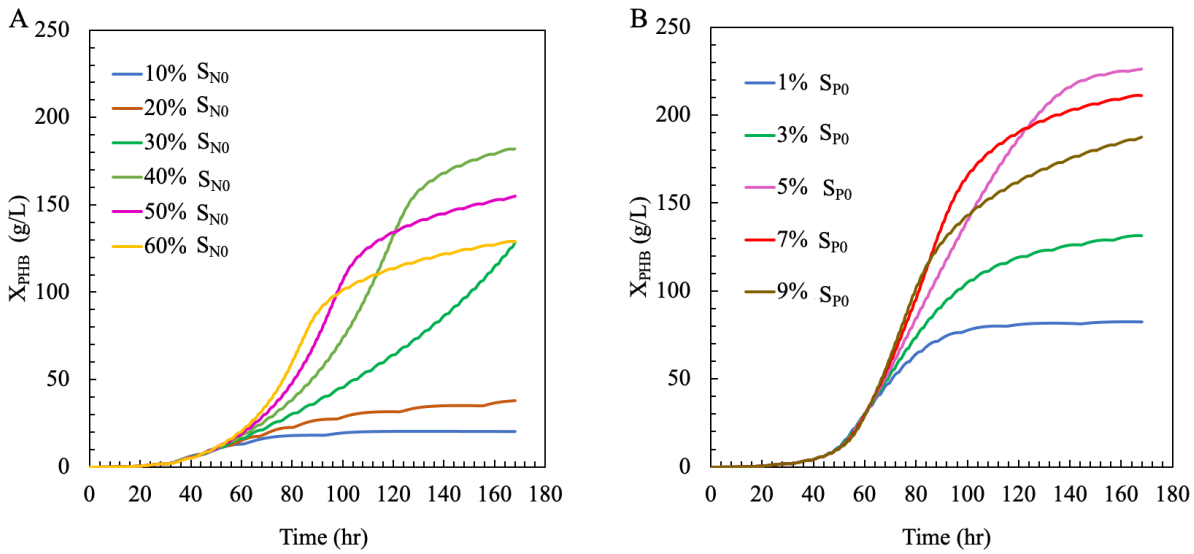

Figure 3-4:Simulated PHB accumulation at the varying amount of nutrient in the medium (A) 1st scenario: nitrogen-limited (B) 2nd scenario: phosphorous limited

The simulated PHB accumulation illustrated in Figure 3-4 also indicated that the medium for repeated fed-batch feeding with limited phosphorous leads to higher PHB accumulation than with limited nitrogen. In the case of limited nitrogen (Figure 3-4 A), the maximum amount of PHB accumulated at 168 hr is 182.0 g/L. In the case of limited phosphorous (Figure 3-4 B), the maximum amount of PHB accumulated at 168 hr is 226.0g/L. Therefore, limiting phosphorus amount in the medium is more favorable to maximize PHB accumulation than limiting nitrogen amount.

The final amount of PHB starts to decrease once the feeding of a nutrient exceeds the optimal amount since the further increase of nutrient feeding increases residual biomass growth rate so that residual biomass hits X_R^{max} when PHB accumulation is still far from reaching its capacity. The more nutrient is supplied in the PHB production phase, the faster residual biomass reaches the cell growth capacity and less PHB is accumulated. As shown in Figure 3-5, f_{PHB} for 7% S_{P0} and 9% S_{P0} are less than $f_{PHB}^{max} = 4$ over the operation, meaning that PHB accumulation has not approached

the production capacity over the operation period. Thus, PHB accumulation is non-stationary for 7% S_{P0} and 9% S_{P0} after the linear phase (Figure 3-4 B).

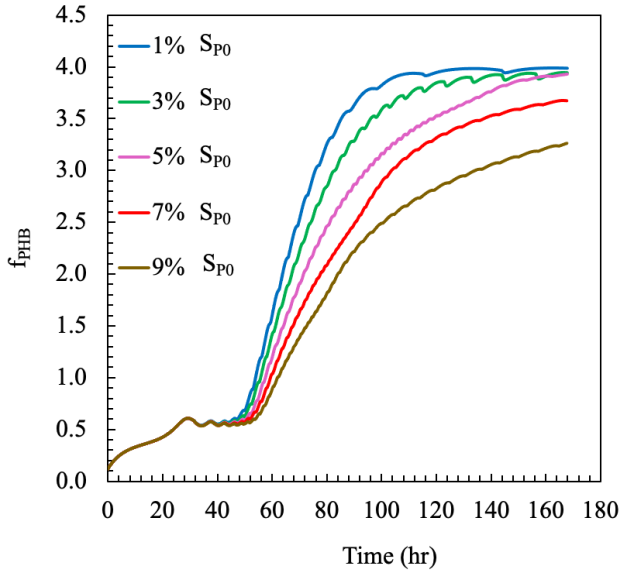

Figure 3-5: f_{PHB} over the operation period at different amount of phosphorous

Figure 3-6 shows the simulated output for all model components under the optimal condition that is fed-batch feeding with limited phosphorous at 5% S_{P0} during the PHB production phase. The PHB production rate is linear when cell growth is maintained by feeding a limited amount of phosphorus until residual biomass reaches the cell growth capacity. After residual biomass hits the X_R^{max}, PHB production starts to slow down, and then PHB accumulation enters the stationary phase. The amount of inert particulate and slowly biodegradable particulate accumulated in the end of the operation are 0.002 g/L and 0.007 g/L respectively, which are negligible compared to the amount of biomass. Thus, inert particulate and slowly biodegradable particulate are not influential components in the PHB production process by pure culture.

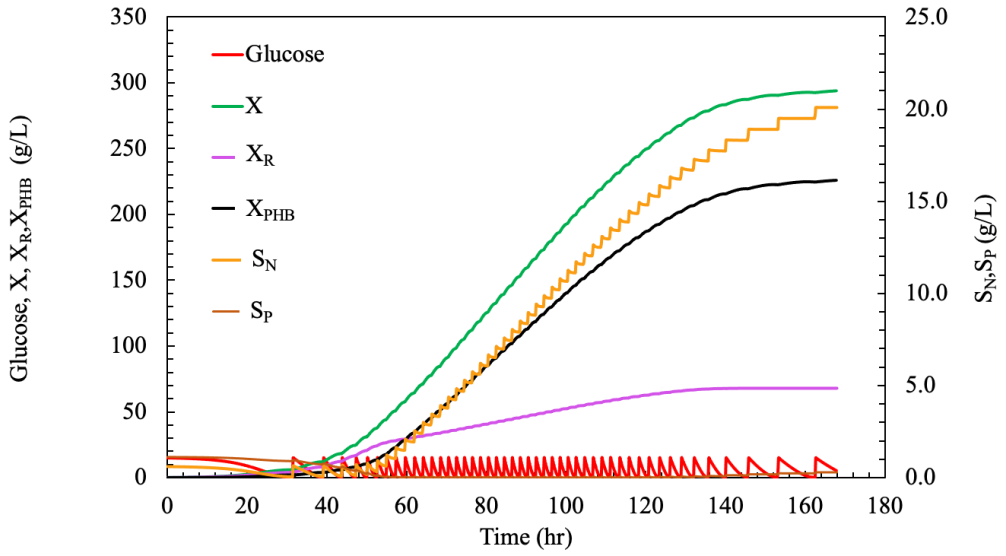

Figure 3-6: Simulation results under optimal condition (the nutrients in the fed-batch feeding medium: 5% S_{P0} and S_{N0})

The Feeding frequency is dependent on nutrient concentration in the feeding medium. The more nutrient concentration supplied during the PHB production phase, the higher feeding frequency. The shortest time between consecutive feedings under the optimal condition in Figure 3-6 is 2 hours. In the case of feeding with 1% S_{P0} and S_{N0}, the shortest time between consecutive feedings is 3 hours. The feeding frequency is a factor to be considered for designing a fed-batch cultivation process. The feeding frequency determines the use of an automated feeding system. In the simulation scenario under the optimal condition, since the operation period is more than 1-day and the shortest time interval for feedings is 2 hours, an automated feeding system is required to accomplish the overnight feedings. Besides, the feeding frequency affects the process control. The process is easier to be controlled with lower feeding frequency. The less frequent feeding provides more time to fix the process if the biomass growth and PHB accumulation go in the wrong direction.

4 Conclusions

The comprehensive numerical model for non-growth-associated PHB production by *Cupriavidus necator* has been developed and calibrated for predicting PHB production and cell growth. The model parameters have been calibrated with 8 selected experimental studies with the goal of using unified values to fit the experimental data among selected studies. The calibrated model shows good agreement with experimental data. After comparing calibrated parameters to reported ranges, unified values of parameters were determined for the present model.

Then, these estimated parameters were used as base values for sensitivity analysis. Sensitivity analysis were conducted by the simple method and by the overall relative sensitivity analysis. μ_S, k_{PHB}, $Y_{X_R/S}$, $Y_{PHB/S}$, Ks, K_N, K_P, i_{NBM}, m_S, and γ were sensitive parameters. These parameters are important to be investigated when studying the kinetics of the PHB production process for a specific bioreactor system. Parameters like max. specific growth rate and yields depend on the experimental conditions of the reactor, so verifying parameters with calculated values based on the experimental measurement is essential to make the model prediction reliable.

Finally, the calibrated model was applied to investigate fed-batch feeding strategies that optimize PHB accumulation. The investigated feeding strategy is fed-batch feeding with a limited amount of one nutrient to maintain cell growth in the PHB production phase. Scenarios of limiting nitrogen and limiting phosphorous were simulated, and the simulation results showed limited phosphorous feeding yields more PHB accumulation than limited nitrogen feeding. In such a feeding strategy, PHB accumulation can be maximized with a limited carbon substrate that is 16 $\frac{g-COD}{L}$ in the fresh medium. The optimal feeding strategy was found to be limited feeding of phosphorous at 5% S_{P0} during the PHB production phase, leading to simulated 226.0 g/L PHB at the end of the 168-hour

operation. The PHB production rate is increased by increasing the amount of the nutrient that keeps cell growth. Such a feeding strategy can make the operation time shorter by increasing the amount of limited nutrient feeding.

The present model calibrated with various studies can be used to control and design the PHB production process for various cultivation conditions. In future research, the model could be improved by calibrating with data from pilot studies or full-scale plants for designing or optimizing full-scale systems for industrial PHB production. More experimental studies could be conducted for measuring sensitive parameters to improve the reliability of the parameters. In terms of feeding strategy investigation, conducting lab experiments according to the model simulated scenarios is essential to investigate the feasibility of the designed feeding strategy. The lab experiments could be designed for the scenarios of nitrogen-limited feeding and phosphorous-limited feeding to verify if the experimental results agree with the simulated results.

References

[1] J. P. Van Der Hoek, H. De Fooij, and A. Struker, "Wastewater as a resource: Strategies to recover resources from Amsterdam's wastewater," *Resour. Conserv. Recycl.*, vol. 113, pp. 53–64, 2016.

[2] G. Mannina, D. Presti, G. Montiel-Jarillo, J. Carrera, and M. E. Suárez-Ojeda, "Recovery of polyhydroxyalkanoates (PHAs) from wastewater: A review," *Bioresour. Technol.*, vol. 297, no. November 2019, p. 122478, 2020.

[3] D. Dionisi, M. Majone, V. Papa, and M. Beccari, "Biodegradable Polymers from Organic Acids by Using Activated Sludge Enriched by Aerobic Periodic Feeding," *Biotechnol. Bioeng.*, vol. 85, no. 6, pp. 569–579, 2004.

[4] Muhammadi, Shabina, M. Afzal, and S. Hameed, "Bacterial polyhydroxyalkanoates-eco-friendly next generation plastic: Production, biocompatibility, biodegradation, physical properties and applications," *Green Chem. Lett. Rev.*, vol. 8, no. 3–4, pp. 56–77, 2015.

[5] P. R. Patnaik, "Perspectives in the modeling and optimization of PHB production by pure and mixed cultures," *Crit. Rev. Biotechnol.*, vol. 25, no. 3, pp. 153–171, 2005.

[6] M. LEMOIGNE, "Produits de Deshydration et de Polymerisation de L'acide β=Oxybutyrique," *Bull. Soc. Chim. Biol.*, vol. 8, pp. 770–782, 1926.

[7] H. Salehizadeh and M. C. M. Van Loosdrecht, "Production of polyhydroxyalkanoates by mixed culture: Recent trends and biotechnological importance," *Biotechnol. Adv.*, vol. 22, no. 3, pp. 261–279, 2004.

[8] C. Kourmentza *et al.*, "Recent advances and challenges towards sustainable polyhydroxyalkanoate (PHA) production," *Bioengineering*, vol. 4, no. 2, pp. 1–43, 2017.

[9] M. G. E. Albuquerque, M. Eiroa, C. Torres, B. R. Nunes, and M. A. M. Reis, "Strategies for the development of a side stream process for polyhydroxyalkanoate (PHA) production

from sugar cane molasses," *J. Biotechnol.*, vol. 130, no. 4, pp. 411–421, 2007.

[10] F. Valentino *et al.*, "Sludge minimization in municipal wastewater treatment by polyhydroxyalkanoate (PHA) production," *Environ. Sci. Pollut. Res.*, vol. 22, no. 10, pp. 7281–7294, 2015.

[11] B. Colombo, T. P. Sciarria, M. Reis, B. Scaglia, and F. Adani, "Polyhydroxyalkanoates (PHAs) production from fermented cheese whey by using a mixed microbial culture," *Bioresour. Technol.*, vol. 218, no. 2016, pp. 692–699, 2016.

[12] L. S. Serafim, P. C. Lemos, R. Oliveira, and M. A. M. Reis, "Optimization of polyhydroxybutyrate production by mixed cultures submitted to aerobic dynamic feeding conditions," *Biotechnol. Bioeng.*, vol. 87, no. 2, pp. 145–160, 2004.

[13] N. Biglari, I. Orita, T. Fukui, and K. Sudesh, "A study on the effects of increment and decrement repeated fed-batch feeding of glucose on the production of poly(3-hydroxybutyrate) [P(3HB)] by a newly engineered Cupriavidus necator NSDG-GG mutant in batch fill-and-draw fermentation," *J. Biotechnol.*, vol. 307, no. October 2019, pp. 77–86, 2020.

[14] S. Y. Lee, "Plastic bacteria? Progress and prospects for polyhydroxyalkanoate production in bacteria," *Trends Biotechnol.*, vol. 14, no. 11, pp. 431–438, 1996.

[15] M. Koller and A. Muhr, "Continuous production mode as a viable process-engineering tool for efficient poly(hydroxyalkanoate) (PHA) bio-production," *Chem. Biochem. Eng. Q.*, vol. 28, no. 1, pp. 65–77, 2014.

[16] N. Tanadchangsaeng and J. Yu, "Microbial synthesis of polyhydroxybutyrate from glycerol: Gluconeogenesis, molecular weight and material properties of biopolyester," *Biotechnol. Bioeng.*, vol. 109, no. 11, pp. 2808–2818, Nov. 2012.

[17] M. S. I. Mozumder, L. Goormachtigh, L. Garcia-Gonzalez, H. De Wever, and E. I. P. Volcke, "Modeling pure culture heterotrophic production of polyhydroxybutyrate (PHB)," *Bioresour. Technol.*, vol. 155, pp. 272–280, 2014.

[18] F. Guzman Lagunes and J. B. Winterburn, "Effect of limonene on the heterotrophic growth and polyhydroxybutyrate production by Cupriavidus necator H16," *Bioresour. Technol.*, vol. 221, pp. 336–343, 2016.

[19] C. Pérez Rivero, C. Sun, C. Theodoropoulos, and C. Webb, "Building a predictive model for PHB production from glycerol," *Biochem. Eng. J.*, vol. 116, pp. 113–121, 2016.

[20] M. Amini, H. Yousefi-Massumabad, H. Younesi, H. Abyar, and N. Bahramifar, "Production of the polyhydroxyalkanoate biopolymer by Cupriavidus necator using beer brewery wastewater containing maltose as a primary carbon source," *J. Environ. Chem. Eng.*, vol. 8, no. 1, p. 103588, 2020.

[21] T. Sugimoto, T. Tsuge, K. Tanaka, and A. Ishizaki, "Control of acetic acid concentration by pH-Stat continuous substrate feeding in heterotrophic culture phase of two-stage cultivation of Alcaligenes eutrophus for production of P(3HB) from CO2, H2, and O2 under non-explosive conditions," *Biotechnol. Bioeng.*, vol. 62, no. 6, pp. 625–631, 1999.

[22] S. Khanna and A. K. Srivastava, "A Simple Structured Mathematical Model for Biopolymer (PHB) Production," pp. 830–838, 2005.

[23] M. Schmidt, J. L. Ienczak, L. K. Quines, K. Zanfonato, W. Schmidell, and G. M. F. de Aragão, "Poly(3-hydroxybutyrate-co-3-hydroxyvalerate) production in a system with external cell recycle and limited nitrogen feeding during the production phase," *Biochem. Eng. J.*, vol. 112, pp. 130–135, 2016.

[24] J. Mozejko-Ciesielska, K. Szacherska, and P. Marciniak, "Pseudomonas Species as

Producers of Eco-friendly Polyhydroxyalkanoates," *J. Polym. Environ.*, vol. 27, no. 6, pp. 1151–1166, 2019.

[25] S. Y. Lee, H. H. Wong, J. Il Choi, S. H. Lee, S. C. Lee, and C. S. Han, "Production of medium-chain-length polyhydroxyalkanoates by high-cell- density cultivation Pseudomonas putida under phosphorus limitation," *Biotechnol. Bioeng.*, vol. 68, no. 4, pp. 466–470, 2000.

[26] M. G. E. Albuquerque, V. Martino, E. Pollet, L. Avérous, and M. A. M. Reis, "Mixed culture polyhydroxyalkanoate (PHA) production from volatile fatty acid (VFA)-rich streams: Effect of substrate composition and feeding regime on PHA productivity, composition and properties," *J. Biotechnol.*, vol. 151, no. 1, pp. 66–76, 2011.

[27] A. Fülöp, R. Béres, R. Tengölics, G. Rákhely, and K. L. Kovács, "Relationship between PHA and hydrogen metabolism in the purple sulfur phototrophic bacterium Thiocapsa roseopersicina BBS," *Int. J. Hydrogen Energy*, vol. 37, no. 6, pp. 4915–4924, 2012.

[28] G. Y. A. Tan *et al.*, "Start a research on biopolymer polyhydroxyalkanoate (PHA): A review," *Polymers (Basel).*, vol. 6, no. 3, pp. 706–754, 2014.

[29] Y. M. Jung and Y. H. Lee, "Utilization of oxidative pressure for enhanced production of poly-β-hydroxybutyrate and poly(3-hydroxybutyrate-3-hydroxyvalerate) in Ralstonia eutropha," *J. Biosci. Bioeng.*, vol. 90, no. 3, pp. 266–270, 2000.

[30] R. Vega and A. Castillo, "A simple mathematical model capable of describing the microbial production of poly(hydroxyalkanoates) under carbon- and nitrogen-limiting growth conditions," *J. Chem. Technol. Biotechnol.*, vol. 93, no. 9, pp. 2564–2575, Sep. 2018.

[31] E. R. Oliveira-Filho, J. G. P. Silva, M. A. de Macedo, M. K. Taciro, J. G. C. Gomez, and

L. F. Silva, “Investigating Nutrient Limitation Role on Improvement of Growth and Poly(3-Hydroxybutyrate) Accumulation by Burkholderia sacchari LMG 19450 From Xylose as the Sole Carbon Source,” *Front. Bioeng. Biotechnol.*, vol. 7, no. January, pp. 1–11, 2020.

[32] M. Koch, K. W. Berendzen, and K. Forchhammer, “On the role and production of polyhydroxybutyrate (Phb) in the cyanobacterium synechocystis sp. pcc 6803,” *Life*, vol. 10, no. 4, 2020.

[33] F. Wang and S. Y. Lee, “Poly(3-hydroxybutyrate) production with high productivity and high polymer content by a fed-batch culture of Alcaligenes latus under nitrogen limitation,” *Appl. Environ. Microbiol.*, vol. 63, no. 9, pp. 3703–3706, 1997.

[34] M. S. I. Mozumder, H. De Wever, E. I. P. Volcke, and L. Garcia-Gonzalez, “A robust fed-batch feeding strategy independent of the carbon source for optimal polyhydroxybutyrate production,” *Process Biochem.*, vol. 49, no. 3, pp. 365–373, 2014.

[35] M. Novak, M. Koller, G. Braunegg, and P. Horvat, “Mathematical modelling as a tool for optimized PHA production,” *Chem. Biochem. Eng. Q.*, vol. 29, no. 2, pp. 183–220, 2015.

[36] N. N. Kulov and L. S. Gordeev, “Mathematical modeling in chemical engineering and biotechnology,” *Theor. Found. Chem. Eng.*, vol. 48, no. 3, pp. 225–229, 2014.

[37] M. Koller *et al.*, “Assessment of formal and low structured kinetic modeling of polyhydroxyalkanoate synthesis from complex substrates,” *Bioprocess Biosyst. Eng.*, vol. 29, no. 5–6, pp. 367–377, 2006.

[38] M. Lopar, I. V. Špoljarić, N. Cepanec, M. Koller, G. Braunegg, and P. Horvat, “Study of metabolic network of Cupriavidus necator DSM 545 growing on glycerol by applying elementary flux modes and yield space analysis,” *J. Ind. Microbiol. Biotechnol.*, vol. 41,

no. 6, pp. 913–930, Jun. 2014.

[39] I. V. Špoljarić *et al.*, "In silico optimization and low structured kinetic model of poly[(R)-3-hydroxybutyrate] synthesis by Cupriavidus necator DSM 545 by fed-batch cultivation on glycerol," *J. Biotechnol.*, vol. 168, no. 4, pp. 625–635, 2013.

[40] E. Heinzle and R. M. Lafferty, "A kinetic model for growth and synthesis of poly-β-hydroxybutyric acid (PHB) in Alcaligenes eutrophus H 16," *Eur. J. Appl. Microbiol. Biotechnol.*, vol. 11, no. 1, pp. 8–16, 1980.

[41] J. H. T. Luong, "Generalization of monod kinetics for analysis of growth data with substrate inhibition," *Biotechnol. Bioeng.*, vol. 29, no. 2, pp. 242–248, 1987.

[42] A. Mulchandani, J. H. T. Luong, and A. Leduy, "Batch kinetics of microbial polysaccharide biosynthesis," *Biotechnol. Bioeng.*, vol. 32, no. 5, pp. 639–646, 1988.

[43] L. Shang, D. Di Fan, M. Il Kim, J. Choi, and H. N. Chang, "Modeling of Poly(3-hydroxybutyrate) Production by Cell Density Fed-batch Culture of Ralstonia eutropha," pp. 417–423, 2007.

[44] L. Marang, M. C. M. van Loosdrecht, and R. Kleerebezem, "Modeling the competition between PHA-producing and non-PHA-producing bacteria in feast-famine SBR and staged CSTR systems," *Biotechnol. Bioeng.*, vol. 112, no. 12, pp. 2475–2484, 2015.

[45] B. J. Ni and H. Q. Yu, "Simulation of heterotrophic storage and growth processes in activated sludge under aerobic conditions," *Chem. Eng. J.*, vol. 140, no. 1–3, pp. 101–109, 2008.

[46] D. M. Hamby, "A Review of Techniques for Parameter Sensitivity," *Environ. Monit. Assess.*, vol. 32, no. c, pp. 135–154, 1994.

[47] M. Henze, W. Gujer, T. Mino, and M. van Loosedrecht, "Activated Sludge Models

ASM1, ASM2, ASM2d and ASM3," *Water Intell. Online*, vol. 5, no. 0, pp. 9781780402369–9781780402369, 2000.

[48] G. Gahlawat and S. K. Soni, "Valorization of waste glycerol for the production of poly (3-hydroxybutyrate) and poly (3-hydroxybutyrate-co-3-hydroxyvalerate) copolymer by Cupriavidus necator and extraction in a sustainable manner," *Bioresour. Technol.*, vol. 243, pp. 492–501, 2017.

[49] J. Marudkla, W. C. Lee, S. Wannawilai, Y. Chisti, and S. Sirisansaneeyakul, "Model of acetic acid-affected growth and poly(3-hydroxybutyrate) production by Cupriavidus necator DSM 545," *J. Biotechnol.*, vol. 268, no. September 2017, pp. 12–20, 2018.

[50] A. Salakkam and C. Webb, "Production of poly(3-hydroxybutyrate) from a complete feedstock derived from biodiesel by-products (crude glycerol and rapeseed meal)," *Biochem. Eng. J.*, vol. 137, no. 2018, pp. 358–364, 2018.

[51] G. Mothes, C. Schnorpfeil, and J. U. Ackermann, "Production of PHB from crude glycerol," *Eng. Life Sci.*, vol. 7, no. 5, pp. 475–479, 2007.

[52] P. Raje and A. K. Srivastava, "Updated mathematical model and fed-batch strategies for Poly-β-Hydroxybutyrate (PHB) production by Alcaligenes eutrophus," *Bioresour. Technol.*, vol. 64, no. 3, pp. 185–192, 1998.

[53] E. Grousseau, E. Blanchet, S. Déléris, M. G. E. Albuquerque, E. Paul, and J. L. Uribelarrea, "Impact of sustaining a controlled residual growth on polyhydroxybutyrate yield and production kinetics in Cupriavidus necator," *Bioresour. Technol.*, vol. 148, pp. 30–38, 2013.

[54] M. Jamilis, F. Garelli, M. S. I. Mozumder, E. Volcke, and H. De Battista, "Specific growth rate observer for the growing phase of a Polyhydroxybutyrate production process,"

Bioprocess Biosyst. Eng., vol. 38, no. 3, pp. 557–567, 2015.

[55] T. Volova, A. Demidenko, E. Kiselev, S. Baranovskiy, E. Shishatskaya, and N. Zhila, "Polyhydroxyalkanoate synthesis based on glycerol and implementation of the process under conditions of pilot production," *Appl. Microbiol. Biotechnol.*, vol. 103, no. 1, pp. 225–237, 2019.

[56] C. Fall, J. A. Rogel-Dorantes, E. L. Millán-Lagunas, C. G. Martínez-García, B. C. Silva-Hernández, and F. S. Silva-Trejo, "Modeling and parameter estimation of two-phase endogenous respirograms and COD measurements during aerobic digestion of biological sludge," *Bioresour. Technol.*, vol. 173, pp. 291–300, 2014.

[57] J. M. L. Dias, L. S. Serafim, P. C. Lemos, M. A. M. Reis, and R. Oliveira, "Mathematical modelling of a mixed culture cultivation process for the production of polyhydroxybutyrate," *Biotechnol. Bioeng.*, vol. 92, no. 2, pp. 209–222, 2005.

[58] L. Belfares, M. Perrier, B. A. Ramsay, J. A. Ramsay, M. Jolicoeur, and C. Chavarie, "Multi-inhibition kinetic model for the growth of Alcaligenes eutrophus," *Can. J. Microbiol.*, vol. 41, no. SUPPL. 1, pp. 249–256, 1995.

Supplementary information

Model calibration with selected experimental studies

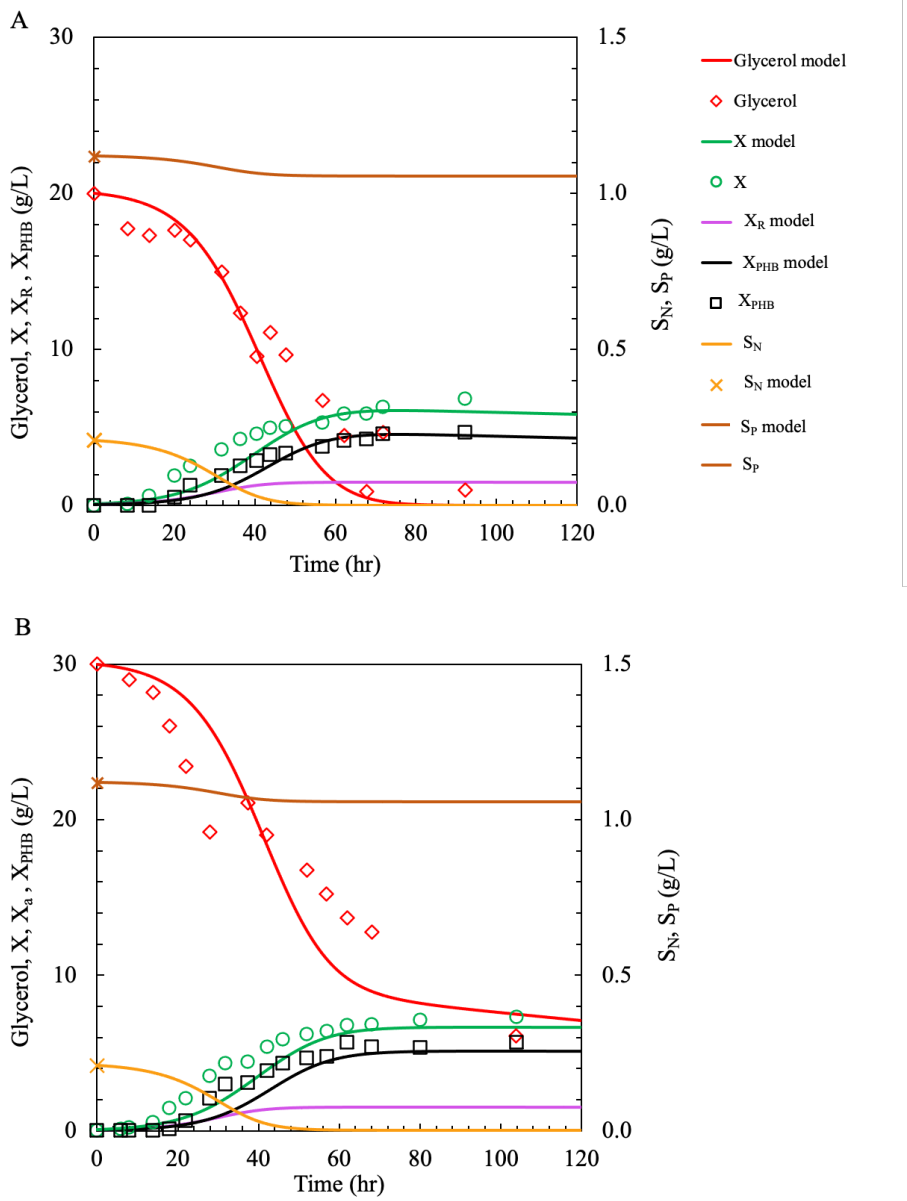

Figure S1: Model calibration with experimental data of Pérez Rivero et al. [19] A. 20 g/L glycerol B. 30 g/L glycerol

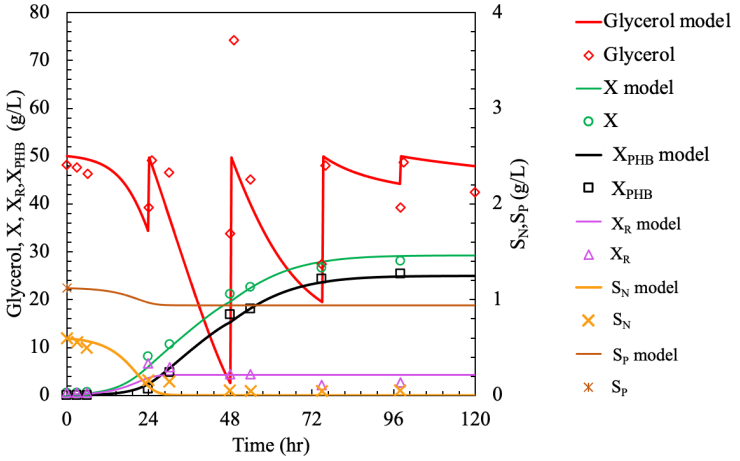

Figure S2: Model calibration with experimental data of Salakkam and Webb [50]

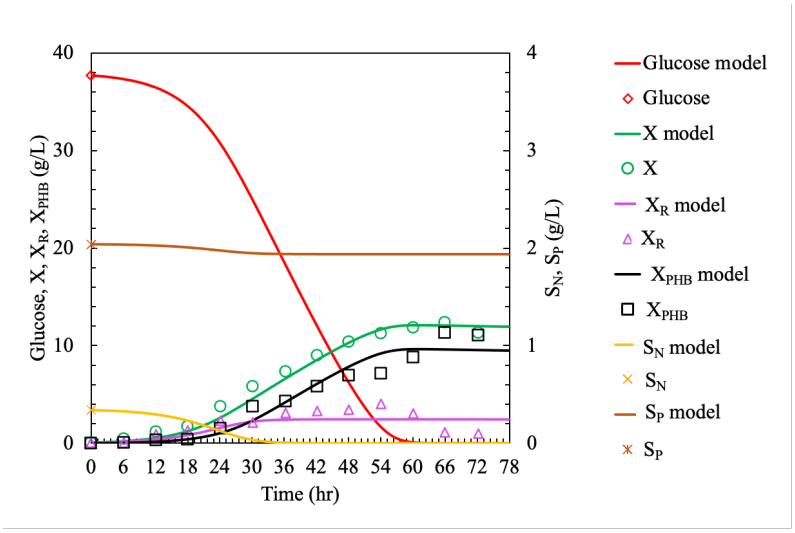

Figure S3: Model calibration with experimental data of Biglari et al. [13]

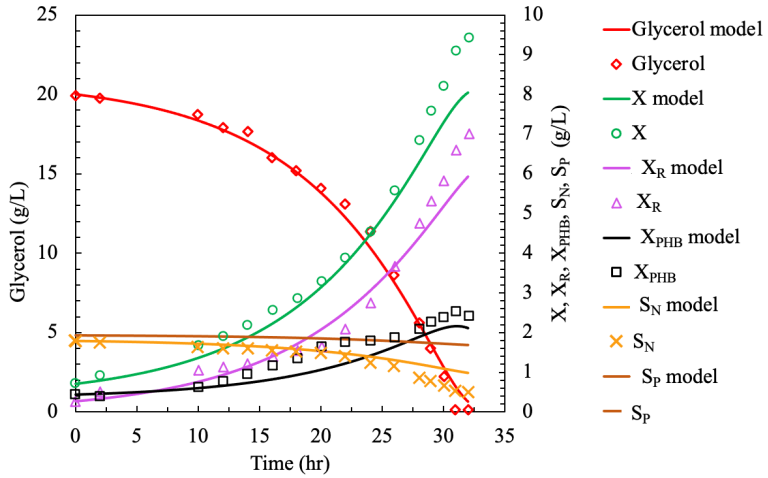

Figure S4: Model calibration with experimental data of Tanadchangsaeng and Yu [16]

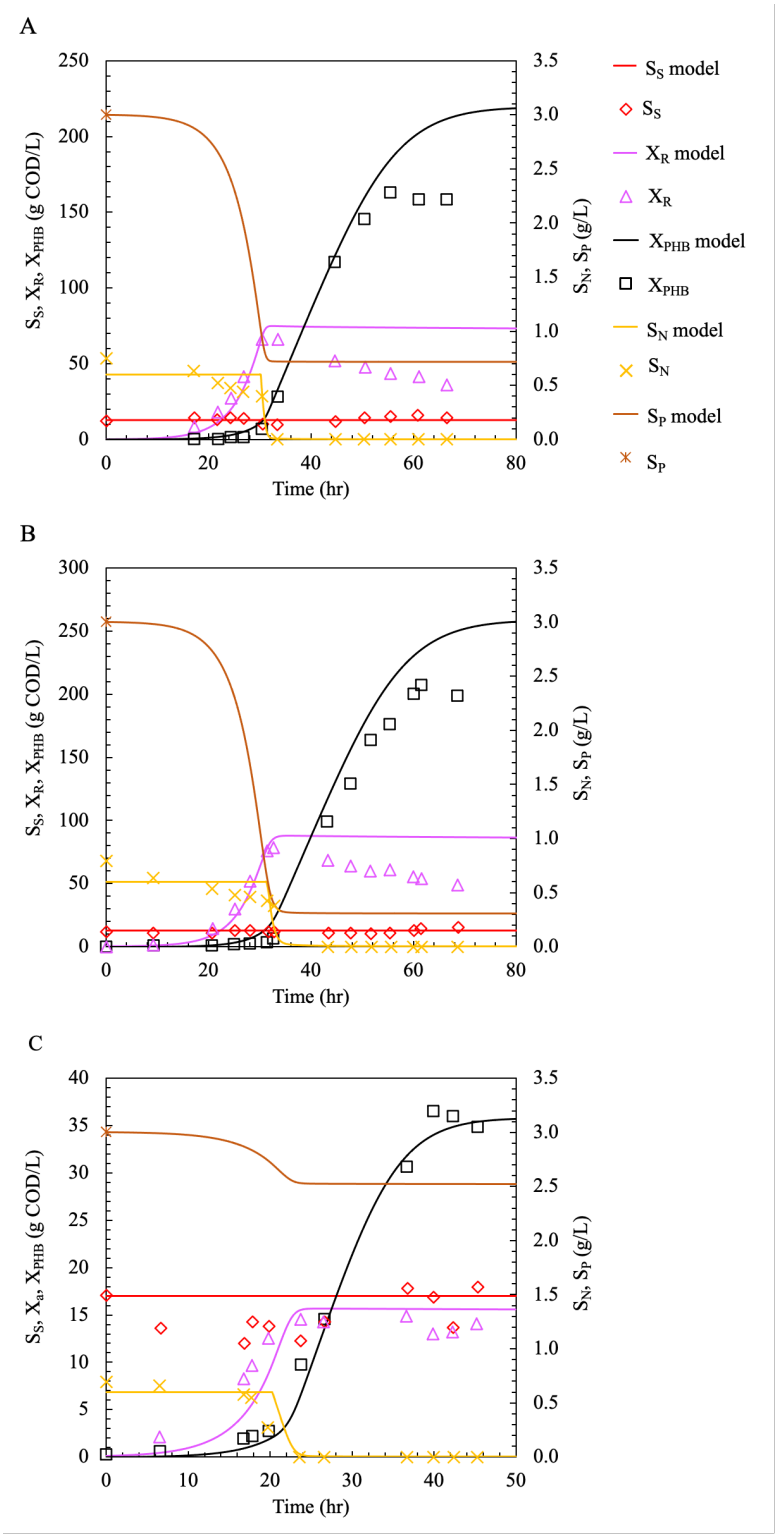

Figure S5: Model calibration with experimental data of Mozumder et al. [17] A. fed with glucose and stop nitrogen feeding at X_R=69 g COD /L B. fed with glucose and stop nitrogen feeding at X_R=79 g COD /L C. fed with glycerol and stop nitrogen feeding at X_R=9.91 g COD/L